

# Effect of gas species on THz generation from two-color lasers

Haiwei Du (杜海伟)<sup>1\*</sup> and Nan Yang (杨楠)<sup>2</sup>

<sup>1</sup>Terahertz Sensing and Imaging Team, Advanced Science Institute, RIKEN, Sendai 9800845, Japan

<sup>2</sup>Laboratory for Laser Plasmas (Ministry of Education) and Department of Physics, Shanghai Jiaotong University, Shanghai 200240, China

\*Corresponding author: haiweidu@yahoo.com

Received January 18, 2013; accepted March 28, 2013; posted online May 30, 2013

The ionization current generated by two-color laser interaction with different gas atoms can produce strong terahertz (THz) emissions. The ionization potential of atoms determines the ionization rate. Thus, THz emission from different atoms varies. Particle-in-cell simulations are conducted to investigate the THz emission from He, Ne, Ar, and N. The THz emissions as a function of the laser field are different because the ionization rate and electron speed depend on the laser field and ionization potential.

OCIS codes: 320.7110, 020.2649, 190.7110, 260.3090.

doi: 10.3788/COL201311.063202.

Laser-produced plasma is a source of strong terahertz (THz) emission<sup>[1–4]</sup>. In particular, the interactions of two-color laser or few-cycle laser pulses with gases are strong THz sources with moderate laser energy and focused laser intensity<sup>[5–8]</sup>. Numerical simulations and experiments suggest that the ionization currents generated during laser propagation in gas targets are mainly from the emission of THz pulses<sup>[9–12]</sup>. The ionization currents are related to the residual momenta of free electrons after laser interaction<sup>[13]</sup>. When a free electron is produced during the ionization process, its canonical momentum is conserved with  $\vec{p}_\perp(t) - e\vec{A}_\perp(t)/c = -e\vec{A}_\perp(t_0)/c$ , where  $t_0$  is the time when the free electron is produced and  $-e\vec{A}_\perp(t_0)/c$  is the residual momentum of the electron. The currents result from the superposition of the current of local individual electrons, as shown by field ionization models such as the Ammosov–Delone–Krainov (ADK) model for tunneling ionization<sup>[14,15]</sup>. In the case of two-color laser or few-cycle laser pulses, the symmetry of the field is lost. High net transverse current is generated along the laser polarization direction, resulting in strong electromagnetic emission at a frequency close to the electron plasma frequency  $\omega_p = (4\pi n_e e^2/m_e)^{1/2}$ , where  $n_e$  is the electron density and  $m_e$  is the electron mass.

Inclusion of particle-in-cell (PIC) simulation with field ionization<sup>[14]</sup> is a useful method that self-consistently models THz emission, as shown in Refs. [10–12,15]. The simulations demonstrated that the phase difference and amplitude ratio had significant effects on the THz emission amplitude in the two-color laser schemes, which was consistent with that detected in the experiment<sup>[16]</sup>. According to the simulations, the optimized ratio of the amplitudes of the two-color lasers for generating a strong THz wave is around  $a_\omega/a_{2\omega} = 1.5$ .

In this letter, we show that THz emission amplitudes and spectra are also strongly dependent on gaseous atom species using PIC simulations. He, Ne, Ar, and N atoms are used as gas targets because they have simple atom structures.

For the two-color laser field,

$$E_L = a_\omega \sin^2\left(\frac{\pi t}{T}\right) \cos\left(\frac{2\pi t}{\tau} + \phi_1\right) + a_{2\omega} \sin^2\left(\frac{\pi t}{T}\right) \cos\left(\frac{4\pi t}{\tau} + \phi_2\right), \quad (1)$$

where  $a_\omega$  and  $a_{2\omega}$  are the normalized amplitudes of the fundamental laser and its second harmonic, respectively, which are related to the laser intensity by  $I = a^2 \times 1.37 \times 10^{18} (\mu\text{m}/\lambda)^2 \text{W}/\text{cm}^2$ ;  $\lambda$  is the wavelength of the fundamental laser in  $\mu\text{m}$ ;  $\tau$  is the period of the fundamental pulse;  $T$  is the duration of the laser pulses;  $\phi_1$  and  $\phi_2$  are the phases of the fundamental laser and its second harmonics, respectively. The two lasers have the same polarization. In our simulation, a fundamental laser wavelength of 1  $\mu\text{m}$  and a phase of zero for the two pulses are used to optimize the THz emission<sup>[15]</sup>. The gas is 20  $\lambda$  long and its atomic density is  $n = 0.0005n_c$ , where  $n_c = m_e \omega^2 / 4\pi e^2$  is the critical density of the plasma electrons for the fundamental laser pulse.

Figures 1(a) and (b) show the plot of the laser field and its vector potential, respectively, when the amplitudes of the fundamental pulse and its second harmonic are  $a_\omega = 0.07$  and  $a_{2\omega} = 0.04$  and the duration of the pulse is  $30\tau$ . The laser field is asymmetrical, which is responsible for the THz emission. We compare the results for He, Ne, Ar, and N atoms as gas targets. The ionization potentials of He, Ne, Ar, and N are presented in Table 1. According to the ADK theory, different atom species have different ionization potentials, and thus, different ionization rates. Given that the residual electron momenta are determined by the vector potential of the laser field at which the

Table 1. Ionization Potential of Some Atoms\*

Potential (eV)	He	Ne	Ar	N
First Order	24.5874	21.5645	15.7596	14.5341
Second Order	54.416	40.962	27.629	29.601
Third Order		63.45	40.74	47.448

\*From www.chemglobe.org.

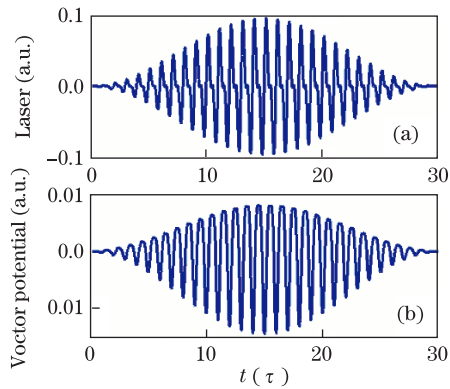


Fig. 1. (a) Two-color laser field and (b) its vector potential. The amplitudes are  $a_\omega=0.07$  and  $a_{2\omega}=0.04$ , respectively, for the two-color laser components.

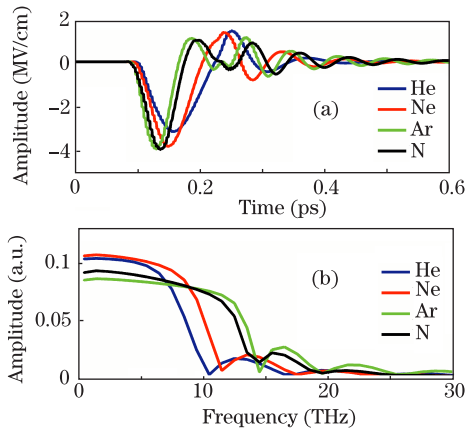


Fig. 2. (a) THz time waveforms and (b) their spectra generated from the ionization current in the gas targets. The laser parameters are the same as those in Fig. 1. The gas target is  $20\lambda$  long.

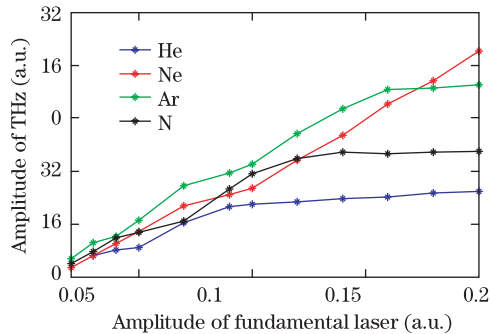


Fig. 3. THz amplitude as a function of the laser amplitude.

electrons are released from the atoms, different ionization potentials also lead to different residual momenta. Figure 2 is the time domain and spectrum of the THz pulses from  $20\lambda$  long gas targets. A low-frequency component is observed in the spectrum (Fig. 2(b)) because the time domain waveform is highly asymmetric in the negative and positive field peaks.

PIC simulations were conducted to explore the THz generation as a function of the laser amplitude. Du *et al.* reported that the ratio of the fundamental laser to its second harmonic affected the THz generation efficiency<sup>[15]</sup>.

Given that the ratio is fixed at  $a_\omega/a_{2\omega}=1.5$ , THz amplitude increases with increasing laser fields  $a_\omega$  and  $a_{2\omega}$ . The results are shown in Fig. 3. Considering the variety of ionization potentials of gas atoms, THz generation for the gas species He, Ne, Ar, and N is different. The scaling of THz emission from different gas atoms is also experimentally explored by Rodriguez *et al.*<sup>[17]</sup>. However, considering that the dispersions of the fundamental laser and its second harmonic are different in different gases, THz emission is affected by relative phase difference and atom species. The simulation shows that the THz emission from He, N, and Ar is saturated. Ne gas shows a different characteristic because its ionization potential is higher.

Plasma density determines the frequency and the amplitude of the electromagnetic wave that it emits. When the density increases from  $0.00005n_c$  to  $0.001n_c$ , the amplitude of the THz pulse increases along with its cosine function, as shown in Fig. 4(a). This result implies that the atom species also affect THz generation. However, the scaling laws for their THz generation are slightly different because the ionization of atoms occurs at a different time of laser pulses. Thus, the electrons from atoms have different speeds. Consequently, the electromagnetic wave from the ionization current is affected. Their frequency bandwidth is broader when the density is bigger, as shown in Fig. 4(b). Ne is used as a gas target, and the same law is observed for He, Ar, and N.

In conclusion, the dependence of THz generation from the ionization current on gas atoms is investigated using PIC simulation. Given that the ionization potential determines the ionization rate of atoms, the current generated by electrons is affected. Therefore, THz radiation varies with different gas atoms. In this study, He, Ne, Ar, and N are used as gas targets. THz emission of the different gases varies depending on the laser field. When gas density increases, THz amplitude increases along with its cosine function and the bandwidth is broader. Considering that the ionizations of the atoms are different, their scaling slightly varies depending on the atom species.

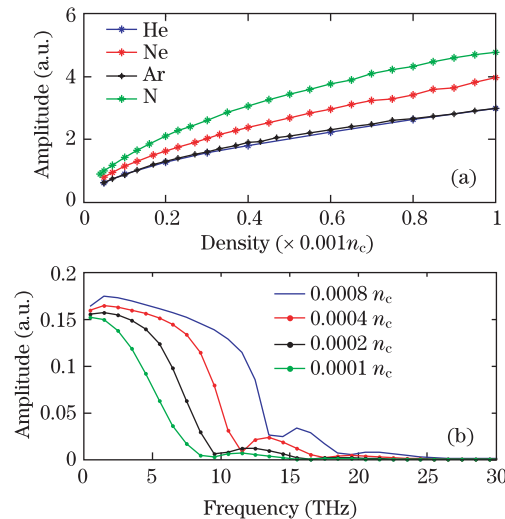


Fig. 4. THz emission as a function of plasma density. When density increases, (a) THz amplitude strength and (b) frequency bandwidth increase. In this study, He is explored as an example.

The simulations in this work were completed in Shanghai Jiaotong University. The authors thank Prof. Zhengming Sheng for the useful discussions. HD is supported by the Foreign Postdoctoral Research Programme of RIKEN, Japan.

## References

1. H. Hamster, A. Sullivan, S. Gordon, W. White, and R. W. Falcone, *Phys. Rev. Lett.* **17**, 2725 (1993).
2. Z. M. Sheng, K. Mima, J. Zhang, and H. Sanuki, *Phys. Rev. Lett.* **94**, 095003 (2005).
3. K. Reimann, *Report Prog. Phys.* **70**, 1597 (2007).
4. W. Fan, *Chin. Opt. Lett.* **9**, 110008 (2011).
5. D. J. Cook and R. M. Hochstrasser, *Opt. Lett.* **25**, 1210 (2000).
6. X. Xu, J. M. Dai, and X. C. Zhang, *Phys. Rev. Lett.* **96**, 075005 (2006).
7. Y. Chen, C. Marceau, W. Liu, Z.-D. Sun, Y. Zhang, F. Théberge, M. Châteauneuf, J. Dubois, and S. L. Chin, *Appl. Phys. Lett.* **93**, 231116 (2008).
8. K. Y. Kim, J. H. Glowina, A. J. Taylor, and G. Rodriguez, *Opt. Express* **15**, 4577 (2007).
9. M. Kress, T. Löffler, M. Thomson, R. Dorner, H. Gimpel, K. Zrost, T. Ergler, R. Moshhammer, U. Morgner, J. Ullrich, and H. Roskos, *Nat. Phys.* **2**, 317 (2006).
10. H. C. Wu, J. Meyer-ter-Vehn, and Z. M. Sheng, *New. J. Phys.* **10**, 043001 (2008).
11. M. Chen, A. Pukhov, X. Y. Peng, and O. Willi, *Phys. Rev. E* **78**, 046406 (2008).
12. W.-M. Wang, Z.-M. Sheng, H.-C. Wu, M. Chen, C. Li, J. Zhang, and K. Mima, *Opt. Express* **16**, 16999 (2008).
13. B. M. Penetrante and J. N. Bardsley, *Phys. Rev. E* **43**, 3100 (1991).
14. M. Chen, Z. M. Sheng, Y. Y. Ma, and J. Zhang, *Chin. J. Comput. Phys.* **25**, 43 (2008).
15. H. W. Du, M. Chen, Z. M. Sheng, and J. Zhang, *Laser Part. Beams* **29**, 447 (2011).
16. M. Kress, T. Löffler, S. Eden, M. Thomson, and H. G. Roskos, *Opt. Lett.* **29**, 1120 (2004).
17. G. Rodriguez and G. Dakovski, *Opt. Express* **18**, 15130 (2010).